The Effect of Grain Size on Flaw Visibility Enhancement Using Split-spectrum Processing

by N. M. Bilgutay and J. Saniie

Abstract

In this paper, experimental data are presented for heat-treated, stainless-steel samples by examining the effects of grain size on the performance of a flaw enhancement algorithm referred to as split-spectrum processing. The principle of this technique is based on partitioning a wide-band received spectrum to obtain decorrelated grain boundary echoes that are subsequently processed to enhance flaw visibility.

Because of their practical importance in welds, large-grained samples in which the sound wavelength is on the order of the grain size were investigated. In such samples, multiple scattering effects can no longer be ignored and may reduce the effectiveness of ultrasonic inspection. The experimental results presented here indicate that, although the split-spectrum processing achieves significant grain noise suppression for large-grained materials, its performance deteriorates as grain size (i.e., scattering) increases.

Nihat M. Bilgutay received a B.S. degree in electrical engineering from Bradley University in 1973 and M.S. and Ph.D. degrees in electrical engineering from Purdue University in 1975 and 1981, respectively. He is currently an assistant professor in the Department of Electrical and Computer Engineering at Drexel University. His research activities and interests include ultrasonic testing and imaging, signal processing, and communication theory. He is a member of Tau Beta Pi, Eta Kappa Nu, Sigma Xi, ASNT, and IEEE.

Jafar Saniie received his B.S. in electrical engineering from the University of Maryland in 1974. In 1977, he received an M.S. in biomedical engineering from Case Western Reserve University and, in 1981, a Ph.D. in electrical engineering from Purdue University. In Sept. 1981, he joined the Applied Physics Research Laboratory to conduct studies in photothermal and photoacoustic imaging. Since Jan. 1983, he has been an assistant professor in the Electrical and Computer Engineering Department at the Illinois Institute of Technology. His research activities and interests include system identification and parameter estimation, digital signal processing, and ultrasonic imaging with both biomedical and industrial application. Saniie is a member of IEEE, Tau Beta Pi, and Eta Kappa Nu.

INTRODUCTION

In many industrial applications, grain echoes become a crucial factor in defect detection. Large grain echoes are observed in ultrasonic examination because of inherent grain characteristics of materials, such as titanium, or because of external factors that result in grain growth, such as in the heat-affected zones of welds.[1] It is a well-known phenomenon that the crystalline structure of metals can be altered by heat treatment, resulting in grain growth.[2] The purity of the material and the method of manufacture determine the heat-treatment temperature and duration that result in grain growth. Although grain growth is undesirable in such applications as welds, it cannot be avoided because of the temperatures to which the heat-treated zone is subjected. As a result of the alteration in grain structure, the ultrasonic examination of the weld region exhibits large grain echoes that can result in "background noise" that masks crucial weld defects.

In ultrasonic examination where the grain size is much smaller than the sound wavelength (Rayleigh scattering), multiple scattering effects can be ignored. However, for a large grain environment in which the sound wavelength is on the order of the grain size (Stochastic scattering), multiple scattering can

no longer be neglected. Therefore, multiple echoes will be received from dominant reflectors, such as flaws, resulting in the reduction of the effectiveness of the ultrasonic inspection. It is thus important to determine the range of grain sizes for which an inspection system is effective. To accomplish this, mples were prepared by using type 303 austenitic stainless-_teel rods to obtain grain sizes similar to the range exhibited by heat-affected zones in welds. The basis for choosing stainless steel for these experiments is its wide use in industrial applications that involve critical welds, such as in nuclear containment vessels, pipings, etc.[3]

EXPERIMENTAL METHODS

A flaw enhancement technique called split-spectrum processing has previously been shown[4,5] to improve flaw visibility in large-grained materials by suppressing grain echoes with respect to the flaw echo. This signal-processing technique was used in conjunction with a random signal flaw detection system that achieves high signal-to-noise ratios by using a correlation type of receiver.[6,7] Thus, the random signal system and the split-spectrum processing algorithm act as two complementary techniques that allow the enhanced detection of flaws in large-grained materials by reducing thermal receiver noise and grain noise, respectively. These properties are especially desirable in the detection and imaging of flaws in large-grained materials with high attenuation, as in welds and titanium samples.

Unlike the random thermal receiver noise, the grain noise is coherent because it results from stationary scatterers within the sample that produce similar echoes for each transmitted pulse. Although these grain echoes resemble noise in the system output, they are actually unwanted signals related to the microstructure and as such cannot be eliminated either by time averaging the received echoes or by using a correlation type of receiver. The split-spectrum technique obtains a decorrelated set of grain boundary echo signals by using a concept similar the frequency diversity principle used in radar.[8-10] Each grain boundary echo signal in this set corresponds to a different range of transmitted ultrasonic frequencies. Because the grains are small and closely spaced, their echoes result in a complicated interference pattern produced by the scatterers. Because the transmitted frequency is varied, there will be significant changes in the interference pattern produced by the grains, whereas the echo from the larger isolated defect present in the sample will remain virtually unchanged. Thus, by processing

the decorrelated echoes corresponding to a set of transmitted signals, the effect of grain echoes can be suppressed with respect to the flaw echo, resulting in flaw-to-grain echo enhancement.[4,5] There are other examples in the ultrasonics literature where this concept has been used.[11,12] However, in the split-spectrum technique, a novel approach was introduced that obtains the frequency diverse signal set from a single wide-band echo signal by digital filtering, thus eliminating the need for individual transmission of each frequency band. The block diagram of this technique is shown in Fig. 1, where the experimental data at the input are obtained using the random signal correlation system.[6,7]

The split-spectrum technique obtains the amplitude spectrum of the echo signal by a fast Fourier transform (FFT) routine, divides the spectrum into the desired number of bands by means of digital filtering, and finally inverse Fourier transforms each band to obtain the frequency diverse signal set. Filtering is accomplished by Gaussian-shaped windows that have a selectable bandwith b and a fixed frequency spacing Δf. The center frequencies of the resulting signals range within the half-power bandwidth of the transducer. These signals are then normalized with respect to amplitude, giving zero-mean outputs with a maximum magnitude of unity. The resulting set of decorrelated signals are then processed to enhance flaw visibility.

The split-spectrum technique described above significantly simplifies the frequency diversity process by eliminating the need for high-frequency filters or equivalent modulation techniques to achieve frequency shifts between transmitted signals. In addition, there is no need to individually sample and store the received signals that correspond to each transmitted frequency. Instead, the same information can be obtained in a single step from the received wide-band signal. Because the filtering in the split-spectrum technique is achieved digitally, processing can be accomplished conveniently for a wide range of processing parameters. Thus, a simple variation in the filter parameters can create a new signal set without requiring additional data collection.

Several techniques have been used for processing the decorrelated signals, including conventional averaging (linear and nonlinear) algorithms and a novel minimization algorithm, as indicated in Fig. 1. In the minimization algorithm, processing involves the selection of the minimum amplitude at each range (data point) from among the set of m squared frequency diverse signals. The mathematical form of both the averaging and the
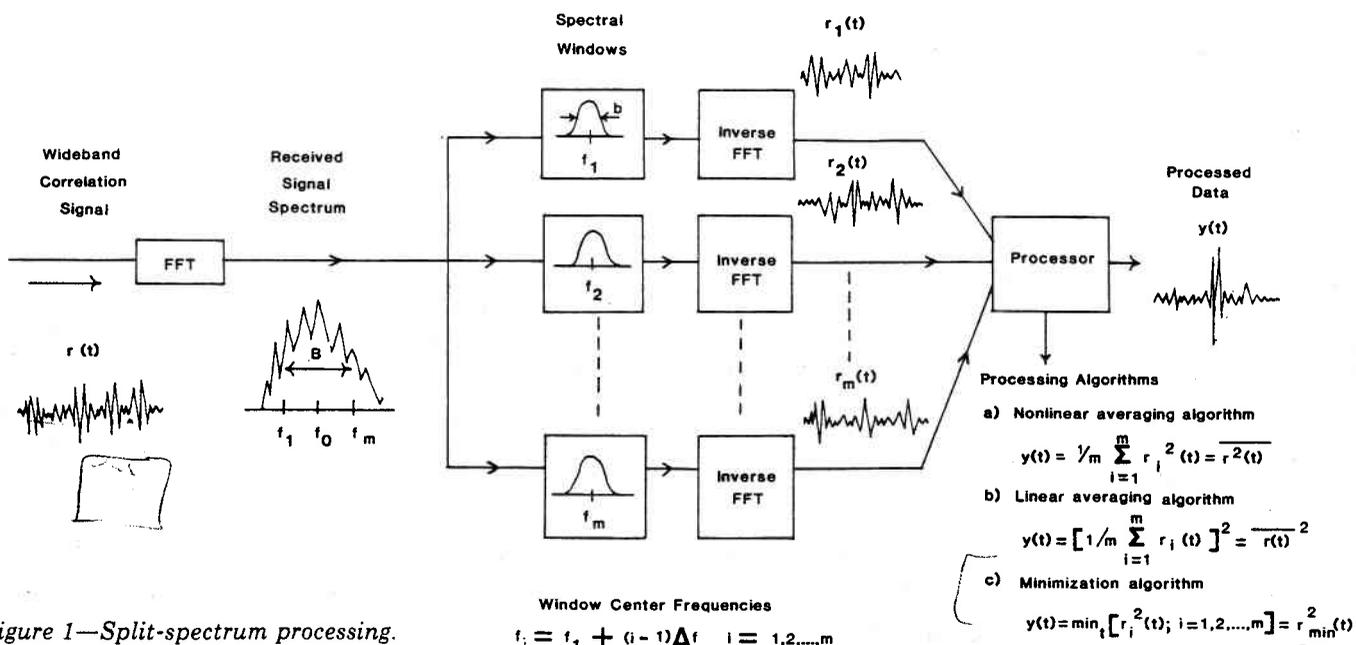

Figure 1—Split-spectrum processing.

Window Center Frequencies

$$f_i = f_1 + (i-1)\Delta f \quad i = 1,2,...,m$$

Processing Algorithms

a) Nonlinear averaging algorithm

$$y(t) = \frac{1}{m} \sum_{i=1}^{m} r_i^2(t) = \overline{r^2(t)}$$

b) Linear averaging algorithm

$$y(t) = \left[\frac{1}{m} \sum_{i=1}^{m} r_i(t)\right]^2 = \overline{r(t)}^2$$

c) Minimization algorithm

$$y(t) = \min_t \left[r_i^2(t); i=1,2,...,m\right] = r_{min}^2(t)$$

minimization algorithms is given in Fig. 1.

Previous experimental data on titanium and stainless-steel samples have shown that, in general, the minimization algorithm achieves significant enhancement in flaw visibility in contrast to the limited improvement observed for the averaging algorithms.[4,5] Therefore, in the work presented here, the minimization algorithm has been used exclusively for signal processing.

The presentation thus far has been introductory in nature to review techniques not only developed earlier but also used in the acquisition and processing of data that are presented here. For a more detailed description and evaluation of these techniques, the reader should refer to the references cited.

In the following sections, the preparation and ultrasonic evaluation of heat-treated stainless-steel samples are presented to determine the effects of grain size on flaw visibility enhancement, in particular, for the minimization algorithm.

SAMPLE PREPARATION

To examine the performance of split-spectrum processing under various grain size conditions, stainless-steel samples that consist of large grains were prepared and tested. The desired range of grain sizes was obtained by heat treating 2 in. (50.8 mm) diameter, type 303 austenitic stainless-steel rods. The chemical contents and impurities in the metal, as well as the mode of manufacture (i.e., extent of hot or cold working due to forging, rolling, or extruding) determine the rate of grain growth.[2] However, because the material properties of the 303 stainless steel that was used were unavailable, several samples were initially heat-treated at temperatures ranging from 800° to 1300°C to determine the grain growth characteristics. The micrographic examination of these samples revealed that noticeable grain growth starts beyond temperatures of 1250°C. On the basis of these results, samples were heat-treated for approximately 1 hour (h) at temperatures of 1325°, 1350°, 1375°, and 1387°C to achieve a range of grain sizes. In each case, the heat-treated samples were quenched rapidly in water.

The final phase of sample preparation involved the selection and preparation of suitably sized flat-bottom holes in the samples. Because heat treatment resulted in hardening of the metal, the holes had to be made initially by an electrodischarge machine and later enlarged by drilling. The hole dimensions were selected so that the ultrasonic echo from both the grains and the hole would be approximately the same. Hole dimensions of 3.18, 3.74, 4.06, and 4.06 mm were obtained for the 1325°, 1350°, 1375°, and 1387°C samples, respectively.

The radial and axial surfaces of the heat-treated samples were examined micrographically to determine the average grain size. The micrographic examination consists of polishing and etching the sample sections and photographically recording their grain structure through a microscope. A micrograph of the stainless-steel sample, heat-treated at 1387°C, is shown in Fig. 2 as an example.

The grain size of the heat-treated samples was analyzed by the intercept method.[13] In this technique, the number of grain boundaries intersected by a fixed point is counted by using a microscope as the sample is moved by a micrometer. The average intercept length is then determined by dividing the total scan distance by the number of grain boundaries. The result of this analysis gives the average spacing between the grain boundaries, which can also be used to calculate the equivalent ASTM grain size number.

The intercept method analysis of the sections from the heat-treated samples resulted in grain size estimates of 75, 86, 106, and 160 μm for the 1325°, 1350°, 1375°, and 1387°C samples, respectively. The grain size estimates correspond to the average of the total data obtained from both the radial and axial surfaces. In addition, to increase the accuracy of the estimates, a grain count was obtained for two perpendicular line segments for each surface.

The grain size estimates given here correspond to the average

RADIAL SURFACE

AXIAL SURFACE

Figure 2—Micrograph of stainless-steel sample heat-treated at 1387°C, magnification at ×128.

grain boundary spacing. However, in the literature, calculations related to scattering are often based on the average grain diameter. A linear relationship exists between the two definitions,[13] given by

$$\overline{D} = k\overline{L}, \qquad (1)$$

where $\overline{D}$ is the average grain diameter, $\overline{L}$ is the average grain boundary spacing (intercept method), and k is a constant multiplier with approximate values between 1.5 and 2.25, depending on the grain shape. This clearly shows that the average grain diameter is an ambiguous term unless the grain shape is known, which is rarely the case. Therefore, it is preferable to define the grain size in terms of the average grain boundary spacing $\overline{L}$. However, based on Equation 1, the average grain diameter in the heat-treated samples may be approximated as twice the average grain boundary spacing for comparison.

The average grain size is often classified in terms of the ASTM grain size number. The following definition[13] relates the average intercept distance $\overline{L}$ to a grain size number g_e, which is approximately equal to that obtained by the ASTM analysis:

(2)
$$g_e = -10.0 + 6.64 \log_{10}(1/\overline{L}),$$

where the unit of $\overline{L}$ is in centimeters (cm). The grain size estimates for the heat-treated samples in terms of the linear intercept values and the corresponding approximation for the ASTM grain size numbers are given in Table 1.

TABLE 1 Grain Size Estimates in Terms of ASTM Grain Size Number.

Sample Heat-treatment Temperature	Linear Intercept Grain Size L (μm)	ASTM Grain Size Number g_e
1325°C	75	4
1350°C	86	4
1375°C	106	3
1387°C	160	2

ATTENUATION OF SOUND WAVES IN MATERIALS

When sound waves are transmitted through a material, the losses in acoustical power result in the attenuation of the initial signal amplitude. The acoustical attenuation is the result of numerous factors, such as absorption, scattering, viscous-damping, and relaxation losses. The acoustical losses are dependent on both material properties (i.e., grain size, crystalline structure, hardness, etc.) and the transmitted frequencies. In general, the amplitude of a plane wave will decay exponentially because of the attenuation in the material and may be written as

(3)
$$A(x) = A_o e^{-\alpha x},$$

where $A(x)$ is the received echo amplitude, A_o is the initial amplitude in the medium, x is the distance traveled by sound, and α is the attenuation coefficient.

The scattering formulas have been studied and classified according to the ratio of the sound wavelength to the average grain size.[14-20] In the Rayleigh region where the sound wavelength is large compared to the mean grain diameter (i.e., $\lambda \gg \overline{D}$), the scattering coefficient varies with the average volume of the grain, fourth power of the wave frequency, and square of the elastic anisotropy. The absorption coefficient, on the other hand, increases linearly with frequency.[14] Therefore, the total attenuation coefficient of ultrasound in the Rayleigh region is expressed as

(4)
$$\alpha = a_1 f + a_2 \overline{D}^3 f^4 \qquad \lambda > 2\pi\overline{D},$$

where a_1 and a_2 are constants, $\overline{D}$ is the average grain diameter, and f is the transmitted frequency. In the Stochastic region where the wavelength is approximately equal to the mean grain diameter, the scattering coefficient varies linearly with the mean grain diameter and with the square of the frequency and elastic anisotropy:

(5)
$$\alpha = b_1 f + b_2 \overline{D} f^2 \qquad \overline{D} < \lambda < 2\pi\overline{D},$$

where b_1 and b_2 are constants. When the wavelength is smaller than the average grain diameter, the scattering coefficient is independent of the frequency, varies inversely with the average grain diameter, and is proportional to the elastic anisotropy. The attenuation coefficient in this case is given by

(6)
$$\alpha = c_1 f + c_2/\overline{D} \qquad \lambda < \overline{D},$$

where c_1 and c_2 are constants. In the Diffusion region, the average grain size is large compared to the wavelength, and the attenuation coefficient is given by

(7)
$$\alpha = (d_1 f + d_2 f^2) + d_3/\overline{D} \qquad \lambda \ll \overline{D},$$

where d_1, d_2, and d_3 are constants and the terms in the bracket correspond to the absorption coefficient. In this region, the absorption losses are much greater, especially because of the thermal losses.

For the experimental applications, the Rayleigh and Stochastic regions defined by Equations 4 and 5 are of primary concern. For these two regions, Papadakis[17] presents scattering coefficient formulas for both cubic and hexagonal crystals, relating the scattering coefficients to the material properties. These formulas are not repeated here but may be referred to for further consideration.

EXPERIMENTAL RESULTS

The heat-treated samples were examined by using the ultrasonic random signal correlation system,[6,7] and the resulting data were processed by the minimization algorithm.[4,5] Prior to applying the minimization algorithm, correlator outputs that correspond to each frequency band (i.e., frequency diverse signals) are squared to remove the negative values.

Figures 3 to 6 show the unprocessed wide-band correlation signals in the squared form, along with the corresponding processed data for the 1325°, 1350°, 1375° and 1387°C samples, respectively. The presentation of the wide-band correlation signals in the squared form is an arbitrary choice that allows a more realistic comparison between the raw and processed data. These results correspond to processing parameters of $\Delta f = 100$ kHz (i.e., frequency spacing between windows), window bandwidths of $b = 300$ kHz (i.e., half-power bandwidth) for the 1375°C, and $b = 350$ kHz for the remaining samples. The window bandwidths used here were experimentally determined to be the optimal choice for the frequency spacing of $\Delta f = 100$ kHz. It
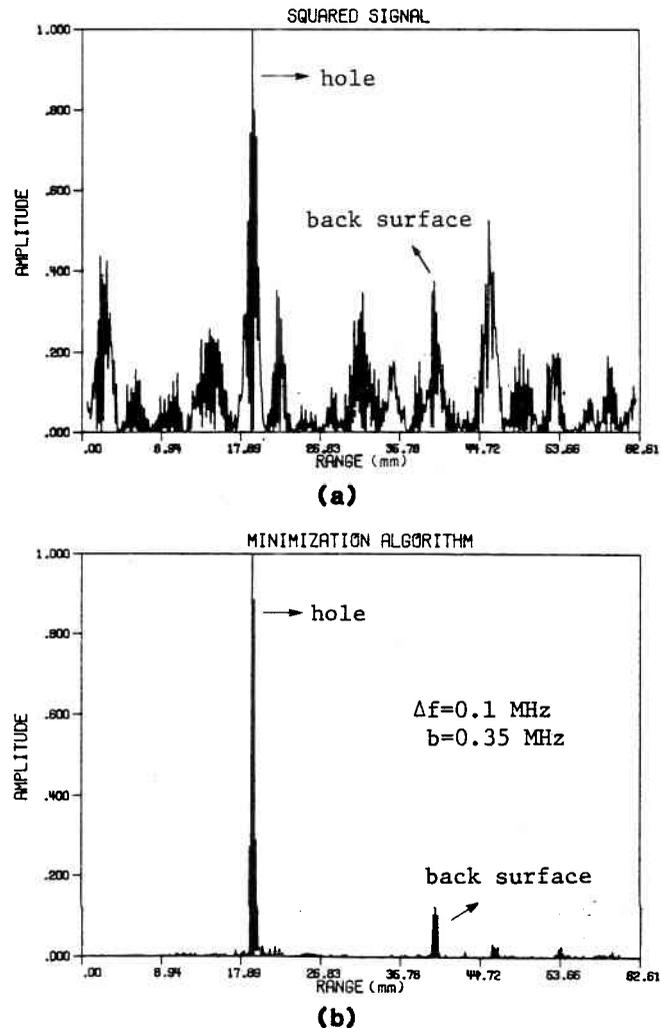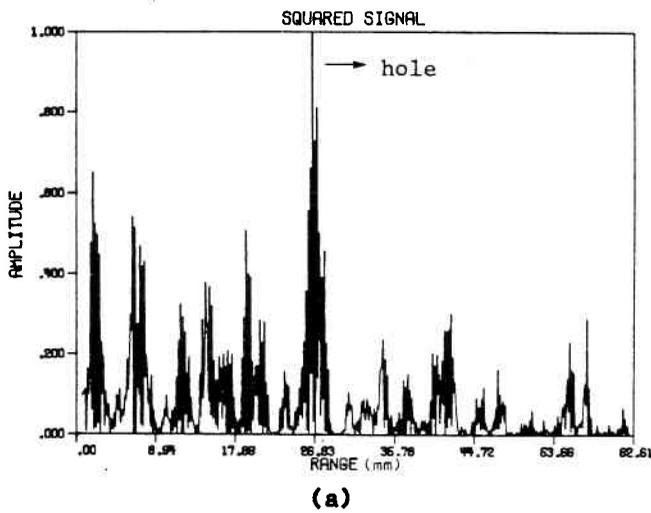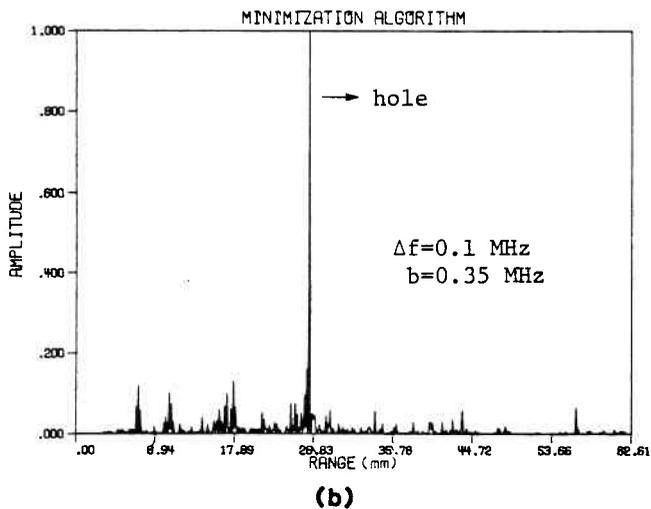

Figure 3—(a) Squared wide-band correlation signal for stainless-steel sample heat-treated at 1325°C. (b) Minimization algorithm output.

Figure 4—(a) Squared wide-band correlation signal for stainless-steel sample heat-treated at 1350°C. (b) Minimization algorithm output.
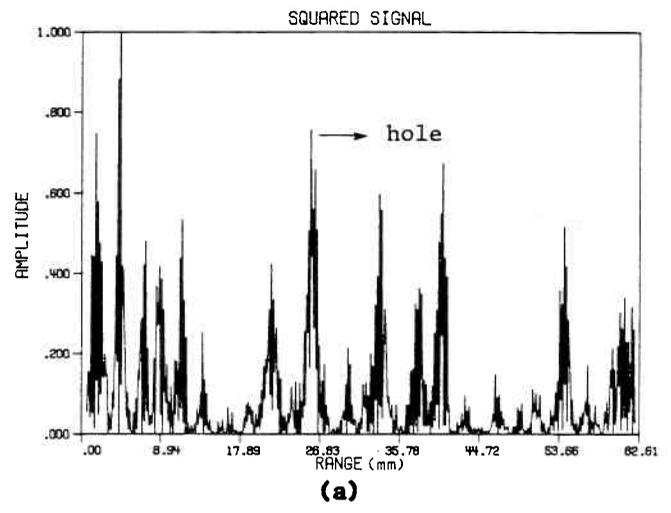

Figure 5—(a) Squared wide-band correlation signal for stainless-steel sample heat-treated at 1375°C. (b) Minimization algorithm output.

should be noted that the performance of the minimization algorithm improves with decreasing Δf, while the flaw enhancement values peak for window bandwidths in the range of 300 to 400 kHz.[4,5] Although additional flaw enhancement can be obtained for smaller values of Δf (i.e., $\Delta f < 100$ kHz), it is not significant enough to warrant increased computation time. Thus, the parameters (i.e., Δf and b) used in Figs. 3 to 6 approximate those that optimize enhancement obtained by the minimization algorithm.
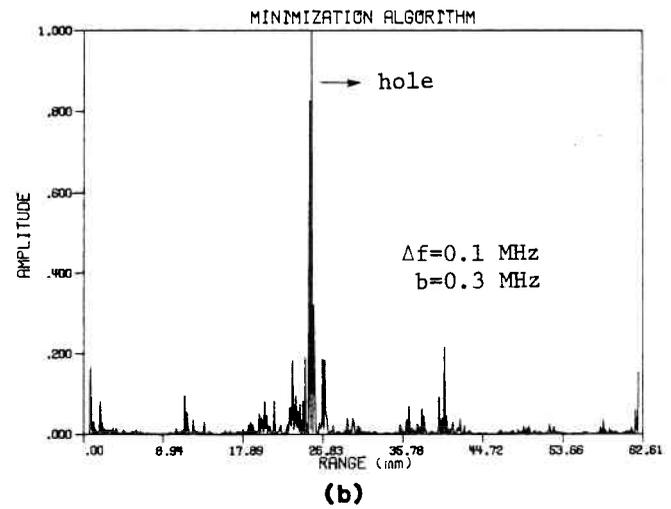
The hole echoes shown in the correlator outputs of Figs. 3 to 6 have amplitudes similar in size to the grain echoes. The processed signals in each case exhibit enhancement in the visibility of the targets. In addition, for the 1325°C sample, the processing recovered the back surface echo, which originally appeared smaller than the neighboring grain echoes seen in Fig. 3. A similar situation is seen for the 1375°C sample in Fig. 5, where the hole echo is smaller than the largest grain echo and is yet easily recovered. These results indicate the capability of the minimization algorithm to distinguish the echo that corresponds to a larger target reflector from grain echoes, even when the target echo appears at or slightly below the grain noise level in the original data.

The enhancement measurement (i.e., $F/G\,|_{enh}$) used throughout this study was based on the improvement in the ratio of the actual flaw to the largest grain echo, which is defined as

(8)
$$F/G\,|_{enh} = \frac{F/G\,|_{out}}{F/G\,|_{in}},$$

where the denominator $F/G\,|_{in}$ is determined from the squared wide-band correlation signal and $F/G\,|_{out}$ is based on the processed output. In some cases, this criterion may result in relatively lower enhancement values compared to criteria based on a reduction in grain variance or mean value. However, because the echo amplitude contains the most significant information in ultrasonic evaluation, this is an appropriate concept for enhancement measurements.

The $F/G\,|_{enh}$ plots for the heat-treated samples are shown in Fig. 7 in terms of window bandwidth b for fixed frequency spacing $\Delta f = 100$ kHz. The peak enhancement occurs at relatively low b values (i.e., $b = 300$ to 350 kHz) for each sample. The lower heat-treatment sample (1325°C) shows steady decay beyond the maximum value as b is increased. The higher heat-treatment samples (1350°, 1375°, and 1387°C) show some fluctuation in $F/G\,|_{enh}$ as b is increased beyond the maximum $F/G\,|_{enh}$ value, which may be a result of increased multiple scattering. However, there seems to be no detectable correlation between grain size and the value of window bandwidth b, where the enhancement reaches maximum, as can be seen from the plots in Fig. 7.

As discussed earlier, the average grain size of the heat-treated samples was determined by using the linear intercept method, which corresponds to the average grain boundary spacing $\bar{L}$. This grain size estimate is linearly related to the grain diameter $(\bar{D})$, with the constant of proportionality determined by the grain shape. For example, this factor is given by 1.5 and 2.25 for spherical and cubic grains, respectively.[13] Because the grain